MedCrave
Step into the World of Research

Physics & Astronomy International Journal

Review Article

Open Access

CrossMark

Analytical comparison of photonic crystal fibers for dispersion compensation with different structures using FDTD method

Abstract

In new generation of optical communication networks, simultaneous transmission of several information channels has become possible over a single optical fiber. But dispersion and dispersion slope of optical fibers are important factors, which limit high capacity optical fiber communication systems to perform high speed transmission.

In this paper, silica core photonic crystal fibers (PCFs) with three and six air–hole rings in the cladding are investigated for effective refractive index, propagation constant and dispersion characteristics, using FDTD method. It is shown that by increasing the number of the air–hole rings in the cladding around the core, the negative dispersion of the PCFs will increase, too. The obtained negative dispersion of –300 ps/nm.km is comparatively high with respect to the published results in the related literature.

Keywords: dispersion, modeling, FDTD method, photonic crystal fibers

Volume 2 Issue 2 - 2018

Faramarz E Seraji, Vajieh Arsang

Department of Communication Technology, Iran Telecom Research Center, Iran

Correspondence: Faramarz E Seraji, Faculty member Optical Communication Group, Department of Communication Technology, Iran Telecom Research Center, Tehran, Iran, Tel +98–21–84977723, Email feseraji@gmail.com

Received: March 26, 2017 | **Published:** April 25, 2018

Introduction

Photonic crystal fibers (PCFs) have attained popularity in designing of compact optical devices utilized in optical networks[1,2] and optical sensing systems.[3,4] The widely used applications are in designing of dispersion compensators commonly used in WDM optical networks reducing the number of required repeaters.[5,6] One of the comparative characteristic features of the PCFs is their flexibilities in response to dispersion effects on propagating pulses present in a long–haul transmission optical fiber line.[7,8]

Till date, the photonic crystal fibers (PCFs) are known to be new types of optical fibers with different structures and profiles as compared to conventional optical fibers that are used in optical communication systems.[9,10] Having different optical characteristics, the PCFs as optical devices have been used in various applications in optical systems, such as super continuum spectrum generation,[11] high optical power transfer,[12] dispersion compensations,[13] tunable optical filters,[14] Erbium–doped optical amplifiers,[15] Bragg grating–based devices,[16] optical nonlinear applications.[17,18]

Different methods are used to evaluate dispersion properties of the PCFs with various structures.[19] In this paper, by using FDTD analysis, two different PCF structures are investigated for utilization in compensations of positive dispersion in optical fiber as a transmission link.

For determination of optimal parameters values of the PCF, analytical and numerical methods, such as the scalar effective index method,[20] the vectorial effective index method (VEIM),[21] the improved vectorial effective index method (IVEIM),[22] and the finite difference frequency domain (FDFD) method,[23,24] are usually utilized. Couple of reports on designs of dispersion compensating fibers (DCFs) are published on optimization of compensation of the dispersions using PCFs in optical transmission bands ranging from 1460 nm to 1675 nm.[25,26]

A survey shows a design of a pentagonal PCF with large flattened negative dispersion by using the full vector finite element method (FEM) where the average negative dispersions for two optimized designs were −611.9 ps/nm/km over 1,460–1,625 nm and −474 ps/nm.km over 1425–1675 nm wavelength bands, respectively.[27] In another report a porous–core circular PCF with circular arrangement of air holes, both in the periodic cladding and the porous core is simulated by using an efficient FEM. It has shown a flattened dispersion of ± 0.09 ps/THz/cm in the frequency range of 0.9–1.3 THz.[28]

An ultra–flattened dispersion over the range of –210 – 15 ps/nm.km is reported in[29] by doping the core of a PCF with Germanium. In another report, a design of a hybrid PCF with elliptical and circular air holes of hexagonal layout with triangular lattice of five rings around the solid core is presented in,[30] where they obtained large flattened dispersion is of the order of 4.88 ps/nm.km over a wavelength range of 1200–1800 nm.

In our previous report, by using two–dimensional finite difference time domain (2D–FDTD), three PCF structures were proposed to optimize the dispersions by considering the effects of the geometrical parameters, such as air–hole diameters and the center–to–center spacing between the holes (pitch). The air–holes were arranged in the cladding in the form of triangular lattice by constituting 11 rings around the core.[31,32]

FDTD numerical method

For a linear, isotropic, non–dispersive material with no source, the time–variant Maxwell's equations are expressed as follows:[9,33,34]

$$\frac{\partial \vec{H}}{\partial t} = -\frac{1}{\mu(r)} \nabla \times \vec{E} \qquad (1)$$

$$\frac{\partial \vec{E}}{\partial t} = \frac{1}{\varepsilon(r)} \nabla \times \vec{H} - \frac{\sigma(r)}{\varepsilon(r)} \vec{E} \qquad (2)$$

Where $\varepsilon(r)$, $\mu(r)$, $\sigma(r)$ are susceptibility, permeability, and conductivity of the dielectric material, respectively, and $\vec{E}$ and $\vec{H}$ are respective electric and magnetic fields vectors. Using Yee cell approach, the Maxwell's equations can be written in the form of partial differential equations with respect to time and space.[35]

If we indicate β as the propagation constant along z direction in a PCF, then the expression $\varphi(x,y,z) = \varphi(x,y)e^{j\beta z}$ will denote component of each field where $j^2 = -1$. Therefore, the differentiation of Maxwell's equations with respect to z may be replaced by $j\beta$ and the fields would be expressed only in terms of transverse components.

A 2D Yee unit cell across the fiber cross section is shown in Figure 1.[35] The $x-$ component of first curl of the Maxwell's equation for magnetic field is derived as:[33]

$$\frac{\partial H_x}{\partial t} = -\frac{1}{\mu}\left(\frac{\partial E_z}{\partial y} - \frac{\partial E_y}{\partial z}\right) \tag{3}$$

By discretization of Equation (3) in terms of time and space and by using Yee cell technique, we obtain:

$$\overrightarrow{H_x}\Big|_{i,k}^{n+1/2} = \overrightarrow{H_x}\Big|_{i,k}^{n-1/2} - \frac{\Delta t}{\mu_{i,k}}\left(\frac{\overrightarrow{E_z}\Big|_{i,k+1}^{n} - \overrightarrow{E_z}\Big|_{i,k}^{n}}{\Delta y} - j\beta\overrightarrow{E_y}\Big|_{i,k}^{n}\right) \tag{4}$$

Where i is the discrete time step, i and k denote grid points of discretization in $xy-$ plane, and Δt, Δx, and Δy denote the time increment, distances between two adjacent points along x and y directions, respectively. Similarly, the components of the other fields can also be derived.

To reduce the computational time, one prefers to consider the real numbers in above equation. For this particular reason, let us consider the real parts of E_z, H_x, and H_y to be $\cos(\beta z + \varphi)$ and that of H_z, E_x, and E_y to be $\sin(\beta z + \varphi)$. Therefore, Equation (4) reduces to:[35]

$$H_x\Big|_{i,k}^{n+1/2} = H_x\Big|_{i,k}^{n-1/2} - \frac{\Delta t}{\mu_{i,k}}\left(\frac{E_z\Big|_{i,k+1}^{n} - E_z\Big|_{i,k}^{n}}{\Delta y} - \beta E_y\Big|_{i,k}^{n}\right) \tag{5}$$

The y and z components of magnetic fields are obtained as follows:

$$H_y\Big|_{i,k}^{n+1/2} = H_y\Big|_{i,k}^{n-1/2} + \frac{\Delta t}{\mu_{i,k}}\left(\frac{E_z\Big|_{i+1,k}^{n} - E_z\Big|_{i,k}^{n}}{\Delta x} - \beta E_x\Big|_{i,k}^{n}\right) \tag{6}$$

$$H_z\Big|_{i,k}^{n+1/2} = H_z\Big|_{i,k}^{n-1/2} + \frac{\Delta t}{\mu_{i,k}}\left(\frac{E_x\Big|_{i,k+1}^{n} - E_x\Big|_{i,k}^{n}}{\Delta y} - \frac{E_y\Big|_{i+1,k}^{n} - E_y\Big|_{i,k}^{n}}{\Delta x}\right) \tag{7}$$

Similarly, one can obtain the components of electrical fields. The stability of the FDTD numerical method is determined by the following expression:[35]

$$\Delta t \le \frac{1}{c\sqrt{\Delta x^{-2} + \Delta y^{-2} + (\beta/2)^{-2}}} \tag{8}$$

For our boundary computational treatment, we use perfectly matched layers method. One of the key characteristic parameters of PCF is chromatic dispersion, which is summation of waveguide and material dispersions. The expression for total dispersion, consisting of material and waveguide dispersion is given as:

$$D_{tot} = -\frac{\lambda}{2\pi c}\left(2\frac{d\beta}{d\lambda} + \lambda\frac{d^2\beta}{d\lambda^2}\right) \tag{9}$$

To simplify the above equation, we define normalized propagation constant $\beta_N (= \beta / k_0 = 2\pi\beta/\lambda)$ and substitute it in (9) to obtain:[9,18,10]

$$D_{tot} = -\frac{\lambda}{c}\left(\frac{d^2\beta_N}{d\lambda^2}\right)\pi \tag{10}$$

Where λ and c are wavelength and velocity of light in a vacuum, respectively. The effective refractive index of fundamental mode is defined as $n_{eff} = \beta(\lambda/2\pi)$.[36]

To evaluate Equation (10) in terms of β_N, $d\beta_N / d\lambda$, $d^2\beta_N / d\lambda^2$, we use FDTD method. The refractive index of the core material is determined by using Sellmeier formula as:[18,37]

$$n_{silica}^2(\lambda) = 1 + \sum_{k=1}^{3}\frac{a_k\lambda^2}{\lambda^2 - b_k^2} \tag{11}$$

Where λ is the wavelength of light, and a_k and b_k are the Sellmeier coefficients. The practical values of b_k and b_k for $k = 1,2,3$ are given as:[38]

$$a_1 = 0.6961663,\ a_2 = 0.4079426,\ a_3 = 0.8974794,$$

$$b_1 = 0.0684043,\ b_2 = 0.1162414,\ b_3 = 9.896161.$$

In this paper, by using the above equations and other related expressions in FDTD method, two PCF samples with different numbers of air–hole rings are selected for design in order to study their dispersion behaviors.

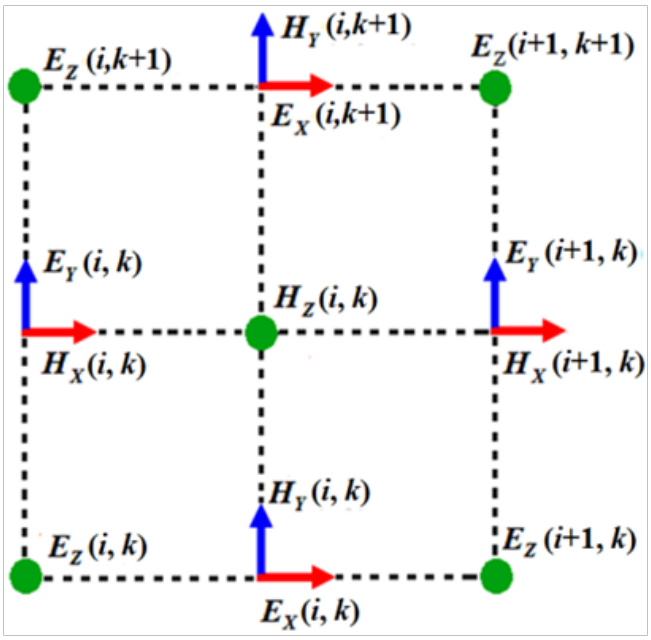

Figure 1 2D yee unit cell across the fiber cross section.[35]

PCF with three rings of air–holes

The selected PCF structure with air–hole of equal diameters $d = 0.75$ μm and air–hole spacing of $\Lambda = 2$ μm arranged in three rings in the form of triangular lattice is illustrated in Figure 2. The core diameter is taken as 1.45 μm .

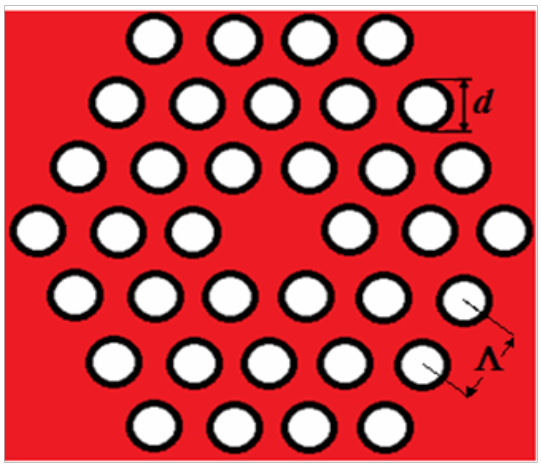

Figure 2 The designed PCF with three rings of air–holes.

The spectrum of chromatic dispersion of fundamental mode in the wavelength range of 1100–2000 nm is illustrated in Figure 3 (Red curve). The dispersion at 1510 nm is obtained as –140 ps/nm.km. The dispersion of the proposed PCF in this case is nearly twice the dispersion of conventional dispersion compensating fiber (i.e.,–80 ps/nm.km).

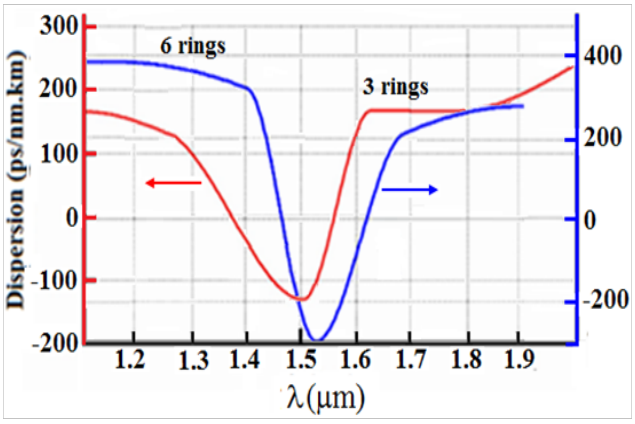

Figure 3 Dispersion spectra of the PCFs with three and six circular air–hole rings in the cladding region.

The PCF with six rings of air–holes

As of previous analysis, a PCF structure is considered with the same air–hole diameter of $d = 0.75$ μm , core diameter of 1.45μm and a different air–hole spacing of $\Lambda = 1.1$ μm . In this case, six air–hole rings are considered in the cladding region (in this case, figure not shown).[36]

By using the home–made programming code, in this case as well, the chromatic dispersion spectrum has been depicted in Figure 3 (Blue curve). In this case, the dispersion value of –300 ps/nm.km is obtained, which twice the value is obtained in the previous design of the PCF with three circular air–hole rings. The results obtained here is comparable to the ones reported,[18] in which the proposed structure with seven air–hole rings were used. The reported dispersion value was –150 ps/nm.km.

In the simulations performed by FDTD method, by varying β values in each case, the resonance fundamental frequencies, wavelengths, and effective refractive indices are determined and tabulated in Table 1.[17,18]

Table 1 Calculated effective refractive index used for determination of dispersion of PCF with six air-hole rings

$\times 10^6 \beta$	n_{eff}	ë (μm)	Fundamental Frequency (THz)
5	1.3010	1.6349	183.50
6	1.3343	1.3973	214.70
7	1.3575	1.2185	246.20
8	1.3745	1.0795	277.90
9	1.3884	0.9631	309.50
12	1.4116	0.7391	405.90
15	1.4239	0.59641	503.00

Conclusion

In this paper, by using FDTD method, two proposed photonic crystal fibers have been analyzed with three and six air–hole rings in the cladding arranged in triangular lattices. In the case of three air–hole rings in the cladding of the PCF, for air–hole with equal diameters $d = 0.75$ μm of and air–hole spacing of $\Lambda = 2$ μm , the dispersion value is determined to be –140ps/nm.km at wavelength 1510nm.

In case of the PCF with six air–hole rings, air–hole spacing of $\Lambda = 1.1$ μm , and with the same air–hole of diameter of $d = 0.75$ μm , the dispersion value is found to be –300ps/nm.km. In both the cases, the diameters of the PCF core are taken as 1.45μm .

It is further shown that when the air–hole spacing Λ is decreased by a ratio of 55% and by doubling the number of air–hole rings, the dispersion will increase more than twice the value. The PCF with high negative dispersion value is suitable for design of high dispersion compensating fiber used in long–haul optical transmission links.

Acknowledgements

The authors greatly acknowledge the allotment of the post–graduate student by GJK Institute of Higher Education, Qazvin, Iran, for collaboration in the running academic project of optical group at ITRC.

Conflict of interest

Authors declare there is no conflict of interest.

References

1. Nielsen MD, Jacobsen C, Mortensen NA, et al. Low–loss photonic crystal fibers for transmission systems and their dispersion properties. *Optics Express*. 2004;12(7):1372–1376.
2. Habib MS, Habib MS, Razzak SMA, et al. Broadband dispersion compensation of conventional single mode fibers using microstructure optical fibers. *Optik: International Journal for Light and Electron Optics*. 2013;124(19):3851–3855.
3. Quintero SMM, Martelli C, Braga AMB, et al. Magnetic field measurements based on terfenol coated photonic crystal fibers. *Sensors*. 2011;11(12):11103–11111.
4. Pinto MR, Lopez–Amo M. Photonic crystal fibers for sensing applications. *Journal of Sensors*. 2012:1–21.
5. Saitoh K, Koshiba M. Chromatic dispersion control in photonic crystal fibers: application to ultra–flattened dispersion. *Optics Express*. 2003;11(8):843–852.
6. Saitoh K, Koshiba M. Numerical modeling of photonic crystal fibers. *IEEE: Journal of Lightwave Technology*. 2005;23(11).
7. Hoo YL, Jin W, Ju J, et al. Design of photonic crystal fibers with ultra–low, ultra–flattened chromatic dispersion. *Optics Communications*. 2004;242(4–6):327–332.
8. Li YF, Wang CY, Hu ML. A fully vectorial effective index method for photonic crystal fibers: application to dispersion calculation. *Optics Communications*. 2004;238(1–3):29–33.
9. Buczynski R. Photonic crystal fibers. *Acta Physica Polonica A*. 2004;106(2):141–168.
10. Sharma KK, Kumar P. On photonic bandgap pcf structures based on pascal's triangle and its propagation characteristics. *International Journal of Advanced Electronics and Communication Systems*. 2012;1(2).
11. Maji PS, Chaudhuri PR. Supercontinuum generation in ultra–flat near zero dispersion PCF with selective liquid infiltration. *Optik: International Journal for Light and Electron Optics*. 2014;125(20):5986–5992.
12. Dianov EM, Bufetov IA, Frolov AA, et al. Fiber fuse effect in microstructured fibers. *IEEE Photonics Technology Letters*. 2004;16(1):180–181.
13. Haque MM, Rahman MS, Habib MS, et al. Design and characterization of single mode circular photonic crystal fiber for broadband dispersion compensation. *Optik*. 2014;125(11):2608–2611.
14. Hoo YL, Ho HL, Jin W, et al. Numerically study of short wavelength filtering of a depressed–index core photonic crystal fiber. *Sensors and Actuators B: Chemical*. 2009;143(1):35–41.
15. Chen W, Li S, Luo W, et al. Fabrication and gain characteristics of the erbium–doped photonic crystal fiber. *Int'l Wire & Cable Symp Proc 60th IWCS Conf*. 2011:346–349.
16. Seraji FE, Anzabi LC, Farsinezhad S. Design of compact long–period gratings imprinted in optimized photonic crystal fibers. *Applied Physics B*. 2009;97(2):425–429.
17. Stone JM. Photonic crystal fibers and their applications in the nonlinear regime. UK: University Of Bath; 2009. p. 1–117.
18. Nozhat N, Granpayeh N. Specialty fibers designed by photonic crystals. *Progress in Electromagnetics Research*. 2009;99:225–244.
19. Li Y, Wang C, Zhang N, et al. Analysis and design of terahertz photonic crystal fibers by an effective–index method. *Applied Optics*. 2006;45(33):8462–8465.
20. Sinha RK, Varshney AD. Dispersion properties of photonic crystal fiber: comparison by scalar and fully vectorial effective index methods. *Optical and Quantum Electronics*. 2005;37(8):711–722.
21. Raja AJ, Porsezian K. A fully vectorial effective index method to analyses the propagation properties of microstructured fiber. *Photonics and Nanostructures–Fundamentals and Applications*. 2007;5(4):171–177.
22. Li Y, Yao Y, Hu M, et al. Improved fully vectorial effective index method for photonic crystal fibers: evaluation and enhancement. *Applied Optics*. 2008;47(3):399–406.
23. Geng Y, Tan X, Wang P, et al. Design of terahertz photonic crystal fibers by finite difference frequency domain method. *Journal of Optics A: Pure and Applied Optics*. 2007;9(11):1019–1023.
24. Seraji FE, Asghari F. Determination of refractive index and confinement losses in photonic crystal fibers using FDFD method: A comparative analysis. *International Journal of Optics and Photonics*. 2009;3(1):1–10.
25. Habib MS, Habib MS, Hasan MI, et al. A single mode ultra flat high negative residual dispersion compensating photonic crystal fiber. *Optical Fiber Technology*. 2014;20(4):328–332.
26. Shaker MM, Majeed MS, Daoud RW. Functioning the intelligent programming to find minimum dispersion wavelengths. *WSEAS Trans Commnu*. 2009;8(2):237–248.
27. Li X, Liu P, Xu Z, et al. Design of a pentagonal photonic crystal fiber with high birefringence and large flattened negative dispersion. *Applied Optics*. 2015;54(24):7351–7357.
28. Islam R, Rana S. Dispersion flattened, low–loss porous fiber for single–mode terahertz wave guidance. *Optical Engineering*. 2015;54(5):1–5.
29. Medjouri A, Mokhtar SL, Ziane O, et al. Investigation of high birefringence and chromatic dispersion management in photonic crystal fiber with square air holes. *Optik–International Journal for Light and Electron Optics*. 2015;12620:2269–2274.
30. Sharma V, Sharma R. Design of hybrid photonic crystal fiber with elliptical and circular air holes analyzed for large flattened dispersion and high birefringence. *Journal of Nanophotonics*. 2016;10(2).
31. Bhattacharya R, Konar S. Design of microstructure fibers with flat negative dispersion over large wavelength bands. *Journal of Optoelectronics and Advanced Materials*. 2008;10(12):3159–3164.
32. Seraji FE, Nouri M. Design of structural parameters of photonic crystal fibers for optimization of dispersion flattening management using FDTD method. *International Journal of Optics and Applications*. 2017;7(3):62–67.
33. Hagness SC. FDTD computational electromagnetic modeling of microcavity. USA: Northwestern University; 1998. p. 1–114.
34. Hoang NM. Two dimensional photonic crystal devices. Netherlands: Delft University; 2012.
35. Qiu M. Analysis of guided modes in photonic crystal fibers using the finite–difference time–domain method. *Microwave and Optical Technology Letters*. 2001;30(5):327–330.
36. Konar S, Bhattacharya R. Design of photonic crystal fibers for dispersion compensation over S, C and L bands. *Optoelectronics and Advanced Materials–Rapid Communications*. 2007;1(9):442–447.
37. Agrawal GP. Nonlinear Fiber optics. 4th ed. USA: Academic Press; 2007.
38. Davison D. Single–mode wave propagation in cylindrical optical fibers. In: Basch EE, editor. USA: Sams Publishing; 1987.